Desalination and Water Treatment
www.deswater.com

doi: 10.1080/19443994.2013.853629

53 (2015) 1361–1370
February

Taylor & Francis
Taylor & Francis Group

Kinetics, isotherm and thermodynamics of tributyltin removal by adsorption onto activated carbon, silica and composite material of silica and activated carbon

Olushola S. Ayanda[a,*], Olalekan S. Fatoki[b], Folahan A. Adekola[c],
Bhekumusa J. Ximba[b], Leslie F. Petrik[a]

[a]*Department of Chemistry, Environmental Nano Sciences Research Group, University of the Western Cape, Private Bag X17, Bellville, South Africa*
Tel. +2348054642362; email: osayanda@gmail.com
[b]*Faculty of Applied Sciences, Department of Chemistry, Cape Peninsula University of Technology, P.O. Box 1906, Bellville, South Africa*
[c]*Department of Chemistry, University of Ilorin, P.M.B 1515, Ilorin, Nigeria*

Received 30 July 2013; Accepted 21 September 2013

ABSTRACT

Activated carbon, silica, and composite material of silica and activated carbon were used as adsorbents to remove tributyltin (TBT) from artificial seawater, and the adsorption efficiencies for the precursors and the composite were compared. The composite presented higher TBT adsorption efficiency than the precursors. The adsorption of TBT onto these materials as a function of adsorbent amount, contact time, pH, stirring speed, initial adsorbate concentration, and temperature was investigated. Maximum TBT adsorption was recorded within the pH range of normal saline water (pH 8). The adsorption kinetics of TBT onto the adsorbents followed a pseudo-second-order kinetic model and the equilibrium adsorption data of TBT onto the precursors and composite were well represented by the Freundlich models. The calculated thermodynamic parameters indicated that TBT adsorption onto the precursor and the composite was spontaneous and endothermic. Optimal conditions for the adsorption of TBT from artificial seawater were applied to TBT removal from natural seawater and the result showed that 99.7, 82.9, and 99.8% TBT was removed by the activated carbon, silica, and composite material, respectively.

Keywords: Organotin compounds; Tributyltin; Activated carbon; Silica; Composite material; Adsorption isotherm; Adsorption kinetics

1. Introduction

Organotin compounds, in particular tributyltin (TBT), are widely used in polyvinyl chloride stabilization, antifouling paints, and biocides [1]. In the marine antifoulant paint market, TBT is used as a biocide in paint formulations. These paints are used to protect the underwater surface area of a ship's hull against barnacles, or algae, in order to avoid increased fuel consumption and premature dry docking [2]. Organotin antifoulants are thus exceptional toxic to non-target marine organism [3]. Studies have also found high

---

*Corresponding author.

concentrations of organotin compounds in the tissues of marine mammals, and the presence of organotin has been linked to mass mortalities of marine mammals [4]. Concerns over the toxicity of these compounds have therefore led to a worldwide ban by the International Maritime Organization. TBT is now considered as a severe marine pollutant. Although tightened controls on the application of organotin antifouling paints to small vessels have been positive in reducing the TBT load to the environment, organotin paints are still applied to large shipping vessels (e.g. tankers and container ships). The release of TBT from these vessels at the shipyard during repairs and painting remains a significant environmental concern.

It is desirable to dispose TBT wastewater after treatment to >99% TBT reduction [5]. Data on the sorption of TBT to nano-oxides, activated carbon, and composite are limited, however, we have reported the kinetics, equilibrium, and thermodynamic studies of TBT adsorption onto activated carbon, fly ash, nZnO, fly ash/activated carbon, and nZnO/activated carbon composites [6,7]. The objective of this study is therefore to evaluate and compare the adsorption potential of activated carbon, silica, and composite material of silica and activated carbon in the removal of TBT from seawater. The effects of adsorbent amount, contact time, pH, stirring speed, initial concentration, and temperature on the adsorption capacity of precursors and the composites have been investigated. Based on these studies, the Langmuir, Freundlich, Temkin, and Dubinin–Radushkevich (D–R) models were used to fit the equilibrium data, and the adsorption kinetics and thermodynamics of TBT were evaluated. Finally, optimal conditions for the adsorption of TBT from artificial seawater were applied to TBT removal from natural seawater.

2. Methods and materials

2.1. Adsorbents and chemical reagents

Activated carbon (100–400 mesh), silica nanopowder (particle size 12 nm), tributyltin chloride (purity 98%), HCl, $NaNO_3$, methanol, hexane, acetic acid, sodium hydroxide, and sodium tetraethylborate ($NaBEt_4$) were purchased from Sigma Aldrich, St. Louis, USA. The composite material of silica and activated carbon in the ratio 1:1 was prepared by the method we reported in Fatoki et al. [8] and Ayanda et al. [9]. The surface and micropore areas of the precursors and the composite were determined by Tristar 3,000 analyzer (Micromeritics Instrument Corporation, Georgia, USA). Carbon, nitrogen, and hydrogen contents were determined by Euro EA3000 elemental analyzer (EuroVector, Redavalle, Italy), and the point of zero charge (PZC) was determined by mass titration. In PZC determination, increasing amounts of sample from 0 to 2.0 g were added to 10 mL of 0.01 mol L^{-1} $NaNO_3$ solution. The resulting pH of each suspension was measured after 24 h. The pH plateau for the highest concentrations of solid in a successful series of mass titrations is taken as the PZC [8]. The physicochemical properties of the precursors and the composite are listed in Table 1. Carbonate, sulphate, and chlorides salts for the preparation of artificial seawater were supplied by Merck (Darmstadt, Germany). A stock solution containing 1,000 mg L^{-1} TBT was prepared by dissolving the organotin compound in methanol, and stored in the dark at 4℃. TBT contaminated artificial seawater samples containing 12.5–100 mg L^{-1} TBT were prepared by spiking artificial seawater with appropriate volume of the TBT stock solution [6,7]. A working solution of derivatization agent was made up daily by dissolving 1.0 g $NaBEt_4$ in 100 mL of methanol while acetate buffer (3 mL acetic acid, 4.0 g sodium acetate, filled up to 1 L with Milli-Q water resulting in a pH of 4.5) was also prepared and stored in a refrigerator.

2.2. Analysis of TBT

The concentration of TBT in the artificial or natural seawater before and after the adsorption studies was determined after derivatization by the addition of 2.0 mL of acetate buffer (pH 4.5) and 1.0 mL of 1%

Table 1
Physicochemical properties of activated carbon, silica, and composite material of silica and activated carbon

Characteristics	Activated carbon	Silica	Silica/ activated carbon
pH	3.30	5.53	3.34
PZC	2.06	4.25	1.74
Surface area (m^2 g^{-1})	1156.6	217.6	605.6
Micropore area (m^2 g^{-1})	442.7	16.1	205.5
Ash content (%)	0.45 ± 0.07	98.3 ± 0.07	52.75 ± 0.07
Carbon content (%)	71.4	0.76	37.95
Nitrogen content (%)	0.35	BD	BD
Hydrogen content (%)	2.82	0.76	2.03

Note: BD—below detection limit.

$NaBEt_4$ and extraction into hexane by horizontal shaking in a separation funnel. The extracts were reduced to 1.0 mL and analyzed by gas chromatography-flame photometric detection (Shimadzu GC-2010 Plus, Shimadzu, Columbia, USA) equipped with a capillary column HP 5 (5% phenyl methyl siloxane, 30 m × 0.25 mm, i.d., film thickness of 0.25 μm, Restek, Bellefonte, USA), and the oven temperature was programed as follows: initially at 60°C hold for 1 min, then heated to 280°C at 10°C min^{-1}, hold for 4 min. The injection and detector temperatures were 270 and 300°C, respectively, and the carrier gas was 99.999% purity helium (Air Liquide, Cape Town, South Africa).

2.3. Adsorption experiments

Adsorption experiment was carried out by shaking 100 mL Erlenmeyer flasks containing 0.5 g of adsorbents and 25 mL of 100 mg L^{-1} TBT contaminated artificial seawater on an orbital shaker (Labotec, Cape Town, South Africa) at 20°C. After 60 min, the aqueous samples were filtered, and the concentrations of TBT in the filtrates were determined. The effects of adsorbent amount, contact time, pH, stirring speed, initial TBT concentration, and temperature on the adsorption capacity of the precursors and the composite were investigated and optimized. Optimum conditions obtained for the adsorption of TBT in artificial seawater were then applied to the sorption of TBT from natural seawater and the result was compared.

2.3.1. TBT uptake capacity

The amount of TBT adsorbed (mg g^{-1}) was calculated based on a general mass balance equation as given in Eq. (1):

$$q = \frac{(c_o - c_e)V}{W} \tag{1}$$

where q is the equilibrium adsorption capacity per gram dry weight of the adsorbent, mg g^{-1}; c_o is the initial concentration of TBT in the solution, mg L^{-1}; c_e is the final or equilibrium concentration of TBT in the solution, mg L^{-1}; V is the volume of the solution, L; and W is the dry weight of the adsorbent, g [10].

Fractional power, pseudo-first-order [11], pseudo-second-order [12], Elovich [11], and intraparticle diffusion rate equations (Eqs. (2)–(6)) have been used for modeling the kinetic of TBT adsorption (Table 2). The Langmuir, Freundlich, Temkin, and D–R isotherms models (Eqs. (7)–(10)) were also used to examine the relationship between the adsorbed and the aqueous concentration at equilibrium (Table 3).

Table 2
Kinetic models used in this study

Kinetic models	Equation	Non-linear form	Integrated form
Fractional power	(2)	$q_t = kt^v$	$\log q_t = \log k + v \log t$
Pseudo-first-order	(3)	$d_q/d_t = k_1(q_e - q_t)$	$\log(q_e - q_t) = \log q_e - k_1 t/2.303$
Pseudo-second-order	(4)	$d_q/d_t = k_2(q_e - q_t)^2$	$t/q = 1/h_o + 1/q_e(t)$ $h = k_2 q_e^2$
Elovich	(5)	$(dq_t/d_t) = \alpha \exp(-\beta q_t)$	$q_t = (1/\beta) \cdot \ln(\alpha/\beta) + (1/\beta). \ln(t)$
Intraparticle diffusivity	(6)	–	$\ln(1 - \alpha) = -k_p t$

Table 3
Isotherm models used in this study

Models	Equation	Non-linear equation	Linear equation
Langmuir	(7)	$q_e = \frac{A_{max} k_L . c_e}{1 + k_L c_e}$	$\frac{c_e}{q_e} = \frac{1}{A_{max} k_L} + \frac{1}{A_{max}} \cdot c_e$
Freundlich	(8)	$q_e = k_F \cdot c_e^{1/n}$	$\log q_e = \log k_F + \frac{1}{n_F} \log c_e$
Temkin	(9)	$q_e = n_T \ln(k_T c_e)$ $n_T = RT/b_T$	$q_e = n_T \ln k_T + n_T \ln c_e$
D–R	(10)	$q_e = q_m \exp(-k_{D-R\varepsilon^2})$ $\varepsilon = RT \ln(1 + 1/c_e)$ $E = 1/\sqrt{2k_{D-R}}$	$\ln q_e = \ln q_m - k_{D-R\varepsilon^2}$

The thermodynamic parameters were determined from the thermodynamic equilibrium constant, K_c. The standard Gibbs free energy ΔG° (kJ mol^{-1}) was calculated using Eq. (11) while the values of the standard enthalpy change ΔH° (kJ mol^{-1}) and standard entropy change ΔS° (JK^{-1} mol^{-1}) were calculated from the intercept and the slope of the linear plot of log K_c versus $1/T$ (Eq. (12)).

$$\Delta G^\circ = -\text{RT} \ln K_c \tag{11}$$

$$\log K_c = \frac{\Delta S^\circ}{2.303\text{R}} - \frac{\Delta H^\circ}{2.303\text{RT}} \tag{12}$$

3. Results and discussion

The result on the effect of adsorbent dose on the adsorption of TBT by the activated carbon, silica, and composite as shown in Fig. 1(a) indicated that the percentage of TBT adsorption increased with increasing adsorbent dose, reaching an optimum at 0.5 g for all the adsorbents, corresponding to 99.7, 87.4, and 99.7% removal by the activated carbon, silica, and composite material of silica and activated carbon, respectively.

The increase in the adsorption capacity with the increasing adsorbent dose is as a result of more adsorptive binding sites due to more adsorbent in the medium at higher dosages. The constant trend in the adsorption capacity after 0.5 g may be due to the saturation of adsorptive binding sites on the adsorbent surface by the TBT molecules [13]. A 0.5 g mass of adsorbent was selected as the optimum adsorbent amount utilized for further studies.

Fig. 1(b) shows the effect of contact time on the adsorption of TBT by the precursors and the composite material. The TBT removal efficiencies at different time intervals ranging from 10 to 70 min were obtained. It was observed that equilibrium was approximately achieved within 60 min. This phenomenon is attributed to the fact that a large number of vacant surface sites are available for adsorption at the initial stage, and after a lapse of time (60 min), the remaining vacant surface sites were difficult to be occupied due to the repulsive forces between the solute molecules on the solid and bulk phases [14]. The adsorption capacity of TBT after 60 min contact time by the activated carbon, silica, and composite material of silica and activated carbon were 4.84, 4.37, and 4.98 mg g^{-1}, respectively.

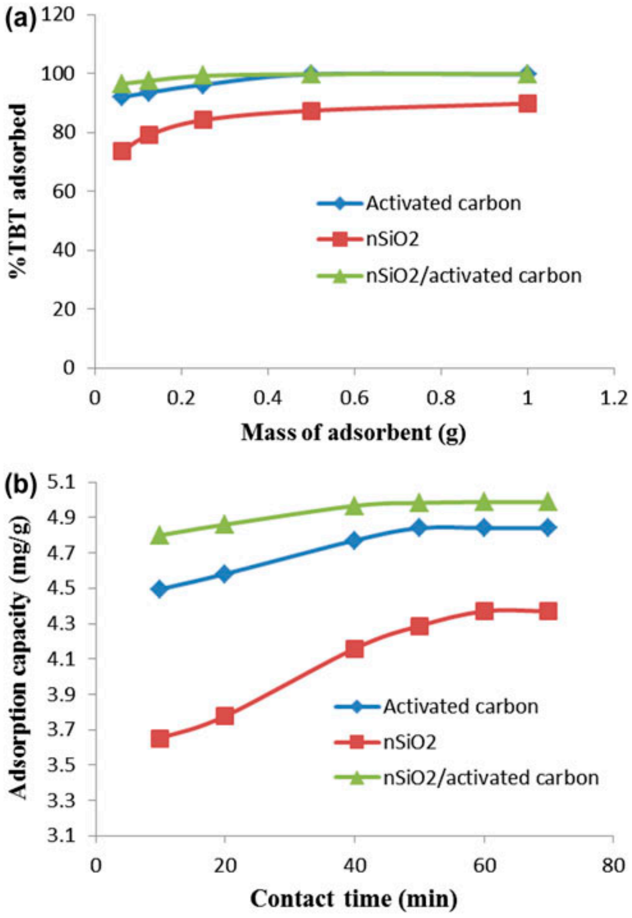

Fig. 1. Effect of adsorbent amount (a) and contact time (b) on the adsorption efficiencies of TBT onto activated carbon, silica, and composite material of silica and activated carbon.
Note: *Experimental conditions:* Concentration of TBT = 100 mg L^{-1}; volume of TBT solution = 25 mL; stirring speed = 160 rpm; temperature = 20°C.

A simple kinetic analysis of the adsorption of TBT on activated carbon, silica, and composite material of silica and activated carbon has been tested according to fractional power model (Eq. (5)), and Table 4 shows the estimated parameters of this model. The results indicated that the power model satisfactorily described the time-dependent of TBT on the precursors and the composite material as the value of the constant v was less than *1*, the regression coefficients were also greater than 0.95.

The kinetic constant k_1 of the pseudo-first-order equation for the adsorption of TBT onto the activated carbon, silica, and composite material of silica and activated carbon is given in Table 4. The results demonstrated that Lagergren model is not applicable in the present case as low regression coefficients (< 0.97) were observed.

Table 4
Kinetic model parameters for TBT adsorption onto the activated carbon, silica, and composite material of silica and activated carbon

Models	Activated carbon	Silica	Silica/ activated carbon
Fractional power			
v (min^{-1})	0.0428	0.1026	0.0037
k_3 (mg g^{-1})	4.0616	2.8451	4.9102
k_3v (mg g^{-1} min^{-1})	0.1738	0.2919	0.0182
R^2	0.9660	0.9685	0.9575
Pseudo-first-order			
k_1 (min^{-1})	0.0216	0.0182	0.04836
q_e (mg g^{-1})	0.5944	1.3858	0.07068
R^2	0.9200	0.9686	0.9450
Pseudo-second-order			
q_e (mg g^{-1})	4.9309	4.5851	4.9950
h_o (mg g^{-1} min^{-1})	4.0650	1.3236	42.3729
k_2 (g mg^{-1} min^{-1})	0.1672		0.06296
1.6983			
R^2	0.9999	0.9992	0.9999
Elovich			
β (g min mg^{-1})	5.0025	2.4331	54.3478
α (g min^2 mg^{-1})	2.712×10^9		1.5266×10^3
4.1081×10^{117}			
R^2	0.9651	0.9656	0.9573
Intraparticle diffusivity			
k_p (min^{-1})	0.0217	0.0181	0.0484
R^2	0.9200	0.9686	0.9450

The results show a very good compliance with pseudo-second-order equation with high regression coefficients (> 0.999) (Table 4). Table 4 shows the adsorption rate constant, k_2, initial adsorption rate, h, and equilibrium adsorption capacity, q_e, of the pseudo-second-order model. The pseudo-second-order kinetic model depends on the assumption that chemisorption may be the rate-limiting step for the adsorption of TBT onto the adsorbents. In chemisorption, the TBT ions stick to the adsorbent surface by forming a chemical (usually covalent) bond and tend to find sites that maximize their coordination number with the surface. The value of h obtained for the pseudo-second-order kinetics increased as follows: 1.3236 mg g^{-1} min^{-1} (silica) < 4.0650 mg g^{-1} min^{-1} (activated carbon) < 42.373 mg g^{-1} min^{-1} (composite material of silica and activated carbon) indicating that activated carbon and the composite material can adsorb TBT more rapidly than silica.

The kinetic constants obtained from the Elovich equation are listed in Table 4. The results do not demonstrate a significant relationship between TBT adsorbed, q_t, and t in these studies with the regression coefficients less than 0.97. In other words, the data does not show satisfactory compliance with the Elovich equation.

The intraparticle coefficients for the adsorption of TBT by the precursors and the composite were also calculated and presented in Table 4. The rate coefficient for particle-diffusion controlled process, k_p, for the sorption of TBT by activated carbon, silica, and composite material of silica and activated carbon are 0.0217, 0.0181, and 0.0484 min^{-1}, respectively.

The pH is a critical factor that affects both the adsorbent and adsorbate chemistry in solution. The effect of pH on the adsorption of TBT onto the adsorbents was studied at pH 3–9. It was observed from Fig. 2(a) that the percentage of TBT adsorbed by the adsorbents steadily increases as the pH of the solution increases from pH 3 to 8, and reaches equilibration at pH > 8. Maximum adsorption capacity was, therefore, recorded within the pH range of normal saline water (pH 8). At low solution pH, the high concentration of H^+ ions promoted the protonation of TBT functional groups, and thus the adsorbents became more positively charged, which inhibits the adsorption of the TBT on it. When the solution pH increased, the solution OH^- concentration increased, which improved the interaction between the adsorbents and the TBT molecules. Therefore, the adsorption capacity of the adsorbents was increased at higher pH value.

Moreover, the results also show that the adsorption capacity of the adsorbents was higher for the adsorbent having the least PZC (composite material of silica and activated carbon) while silica with the highest PZC has the least TBT adsorption capacity. For the composite, adsorption of TBT is high because the surface of the precursors become negatively charged at pH exceeding from these PZC which listed in Table 1 up to pH 9.5, which facilitated the attraction of TBT to the negative activated carbon, silica, and composite surface. About 96.9, 87.9, and 99.7% of TBT were removed by the activated carbon, silica, and composite material, respectively, at a contact time of 60 min, stirring speed of 160 rpm and a temperature of 20°C. The order of decreasing adsorption capacity was thus: composite material of silica and activated carbon > activated carbon > silica.

The stirring speed of the adsorption process was also studied and optimized. The stirring speed on the adsorption of TBT onto the adsorbents was studied at a stirring speed of 160–200 rpm. The adsorption

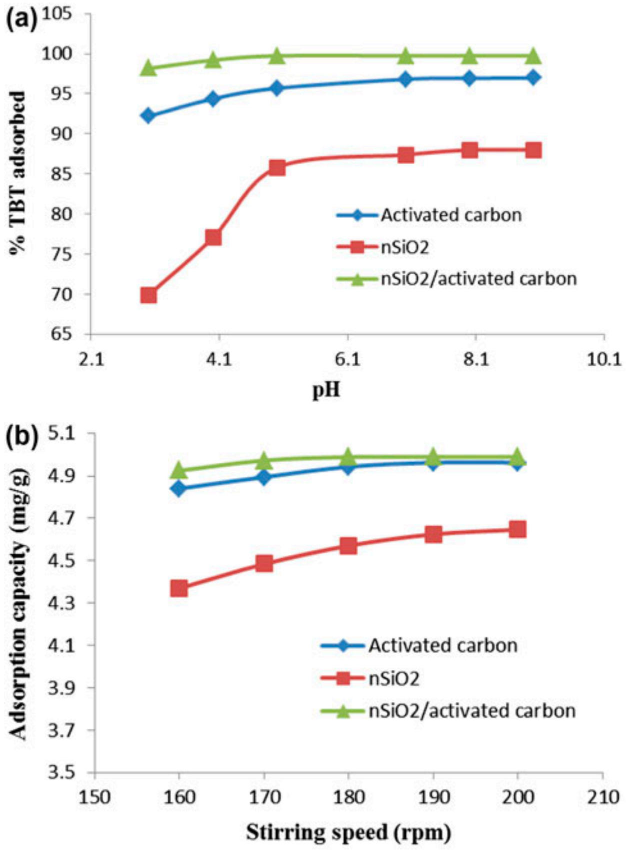

Fig. 2. Effect of pH (a) and stirring speed (b) on TBT adsorption onto activated carbon, silica, and composite material of silica and activated carbon.
Note: *Experimental conditions:* Concentration of TBT = 100 mg L^{-1}; volume of TBT solution = 25 mL; mass of adsorbent = 0.5 g; contact time = 60 min; temperature = 20˚C.

capacity of the adsorbents, therefore, increases as the stirring speed of the mixture increases from 160 to 190 rpm after which equilibration was attained (Fig. 2(b)). This could be explained that the pores on the surface of the adsorbents were unrestricted at high stirring speed making all the pores available for adsorption until saturation was reached at 190–200 rpm. Furthermore, according to Alslaibi et al. [15], the resistance of the boundary layer surrounding the adsorbate weakens at strong agitation rates. Maximum amount of 4.96, 4.65, and 4.989 mg g^{-1} of TBT were removed from 100 mg L^{-1} TBT by the activated carbon, silica, and composite, respectively, at a contact time of 60 min, pH 8, temperature of 20˚C, and a stirring speed of 200 rpm (Fig. 2(b)). The order of decreasing adsorption capacity was: composite material of silica and activated carbon > activated carbon > silica.

The adsorption of TBT on activated carbon, silica, and composite material of silica and activated carbon increased as the initial TBT concentration increased from 12.5 to 100 mg L^{-1}, indicating that adsorption is also favorable for the higher TBT concentrations that have been investigated. The increase in the adsorption capacity with an increase in initial TBT concentration is a result of the increase in driving force due to the concentration gradient developed between the bulk solution and the surface of the adsorbents [16]. At higher concentration of TBT, the active sites of the adsorbents were surrounded by much more TBT and the process of adsorption continues, leading to an increased uptake of TBT from the solution. Therefore, the values of q_e increased with the increase in the initial TBT concentrations.

The Freundlich model [17] is originally empirical in nature but was later interpreted as adsorption to heterogeneous surfaces or surfaces supporting sites of varied affinities and has been used widely to fit experimental data [18]. The present study results indicate that the Freundlich model fits the experiment data well (Table 5). It is the suitable model for describing these adsorption processes, as R^2 values are generally higher than other models, probably due to the real heterogeneous nature of the surface sites involved in the process of adsorption. The value of k_F determines

Table 5
Isotherms constants for the adsorption of TBT onto the activated carbon, silica, and composite material of silica and activated carbon

Equilibrium models	Activated carbon	Silica	Silica/activated carbon
Freundlich			
k_F (mg g^{-1} (L $mg^{-1})^{1/n}$)	6.6589	0.5882	36.12
n_F	0.8375	0.9508	0.7401
R^2	0.9977	0.9994	0.9927
Langmuir			
k_L (L mg^{-1})	−0.2494	−0.00764	−1.3142
A_{max} (mg g^{-1})	−19.0476	−78.74	−10.1317
R^2	−0.00764	0.4777	0.6799
Temkin			
n_T (L g^{-1})	3.8895	3.1893	4.4654
k_T (mg L^{-1})	6.1492	0.8396	17.1936
b_T (J mol^{-1})	626.30	763.80	545.53
R^2	0.8899	0.8851	0.9010
Dubinin–Radushkevich			
k_{D-R} (J^2 mol^{-2})	8×10^{-8}	7×10^{-7}	5×10^{-8}
q_m (mg g^{-1})	8.1858	4.871	14.8634
E (J mol^{-1})	2,500	845.15	3,162.28
R^2	0.9279	0.7990	0.9772

the adsorption capacity of adsorbent at equilibrium concentration in a solution [19]. A higher k_F value therefore corresponds to a higher adsorption capacity. According to the k_F values listed in Table 5, the adsorption capacity of TBT is higher for the composite material of silica and activated carbon than for activated carbon, and activated carbon is in turn higher than for silica. The value of n_F, for all the adsorbents, falling in the range 1–10 indicates favorable adsorption.

The experimental data (Table 5) does not fit the Langmuir model, as the R^2 values are very low (<0.68). Temkin and D–R isotherm models give low R^2 value (<0.91 for Temkin; <0.98 for D–R) and can also not be used to describe the adsorption processes.

The experimental result obtained on the effect of temperature shows that the adsorption capacity of TBT onto all the adsorbents increases with increase in the solution temperature (Fig. 3(a)). This indicates that the adsorption of TBT onto the precursors and the composite is endothermic. The increase in the rate of adsorption with the increase in temperature may be attributed to the strong adsorptive forces between the active sites of the adsorbents and adsorbate species and also between the adjacent molecules of the adsorbed phases.

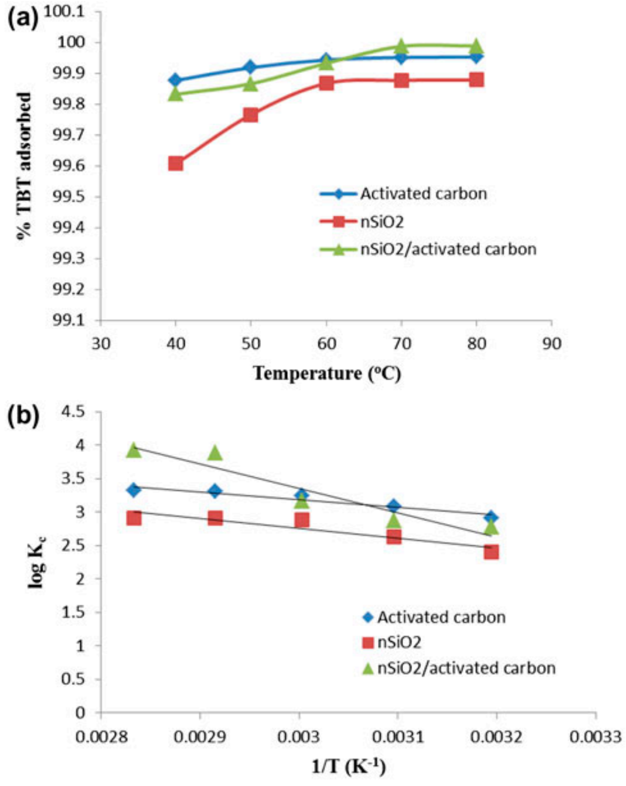

Fig. 3. Effect of temperature (a) and Van't Hoff plot (b) for TBT adsorption onto activated carbon, silica, and composite material of silica and activated carbon.
Note: *Experimental conditions:* Concentration of TBT = 100 mg L^{-1}; volume of TBT solution = 25 mL, mass of adsorbents = 0.5 g; contact time = 60 min; pH = 8; stirring speed = 200 rpm.

Approximately, 99.9, 99.8, and 99.9% of TBT were removed by activated carbon, silica, and composite material of silica and activated carbon, respectively, at a contact time of 60 min, pH 8, and a stirring speed of 200 rpm. The order of increasing adsorption capacity was thus: silica < activated carbon ≈ composite material of silica and activated carbon.

Fig. 3(b) shows the Van't Hoff plot [20] for the adsorption of TBT and the variation in the extent of adsorption with respect to temperature has been explained on the basis of the change in enthalpy (ΔH°), change in entropy (ΔS°), and change in free energy (ΔG°) as shown in Table 6.

The positive values of ΔH° for the intervals of temperatures also showed the endothermic nature of the adsorption process. The positive values of ΔS° correspond to an increase in degree of freedom of the adsorbed TBT and suggest the increase in concentration of adsorbate in solid–solution interface indicating an increase in adsorbate concentration onto the solid phase. It is evident from Table 6 that ΔG° values were found to be more negative as the

Table 6
Thermodynamic parameters for the adsorption of TBT onto the activated carbon, silica, and composite material of silica and activated carbon

Temperature (℃)	ΔG° (kJ mol^{-1})	ΔS° (JK^{-1} mol^{-1})	ΔH° (kJ mol^{-1})	K_c
Activated carbon				
40	−17.434	127.830	22.293	812.0
50	−19.080			1,218.5
60	−20.679			1,753.4
70	−21.731			2,039.8
80	−22.425			2,082.3
Silica				
40	−14.40	136.402	27.861	253.45
50	−16.26			4,226.4
60	−18.33			750.88
70	−19.11			812.01
80	−19.69			818.67
Silica/activated carbon				
40	−16.62	273.364	69.709	594.2
50	−17.76			745.3
60	−20.19			1,469.6
70	−25.52			7,691.3
80	−26.50			8,332.3

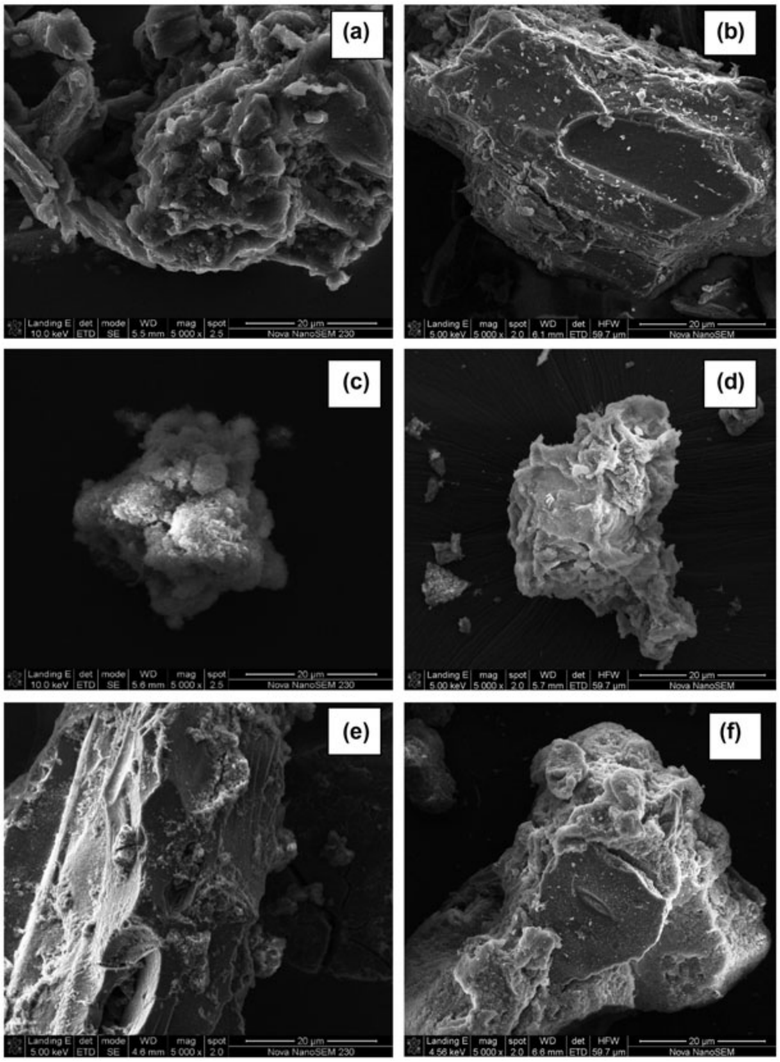

Fig. 4. SEM of activated carbon before (a) and after (b) TBT adsorption; silica before (c) and after (d) TBT adsorption; and composite material of silica and activated carbon before (e) and after (f) TBT adsorption.

temperatures increases, this indicated that the adsorption efficiency of TBT onto the precursors and composite increases with increase in temperature.

The SEM analysis of the adsorbents before and after the adsorption studies is as shown in Fig. 4. The micrographs show that the smooth surfaces of the adsorbents were clearly seen before adsorption but the surface morphologies were all changed after adsorption.

4. Practical application of TBT adsorption to natural seawater condition

Optimal conditions for the adsorption of TBT from artificial seawater were applied to TBT removal from contaminated natural seawater obtained from Cape Town harbor. The physicochemical properties of the seawater are: TDS (18.78 ppt), salinity (22.65 psu), turbidity (3.26 NTU), pH (7.5), conductivity (37.56 mS cm^{-1}), resistivity (26.60 Ω), and 4.615 mg L^{-1} TBT concentration. The percentage of TBT removed after adsorption of TBT in 25 ml of contaminated natural seawater by 0.5 g of adsorbent, contact time of 60 min, and stirring speed of 200 rpm under natural condition are 99.7, 82.9, and 99.8% by the activated carbon, silica, and composite material of silica and activated carbon, respectively.

Although the composite material of silica and activated carbon has lower BET surface area than activated carbon, but has a slightly higher adsorption capacity. The higher adsorption capacity and removal efficiency of the composite material has been attributed to improvement in the physicochemical properties as well as the combination of the adsorption characteristic of activated carbon with the catalytic properties of oxide contained in the composite material [6,7]. A comparison of the results obtained with previous works showed that the precursors namely: activated carbon, fly ash, nZnO, and $nSiO_2$ was able to remove 99.7, 94.2, 80.4, and 82.9% TBT, respectively, while composite materials of fly ash and activated carbon, nZnO and activated carbon, and silica and activated carbon removed 99.8, 99.88, and 99.8% TBT, respectively, from contaminated natural seawater.

5. Conclusion

The adsorption performances of activated carbon, silica, and composite material of silica and activated carbon are studied in terms of kinetic and adsorption isotherms for the removal of TBT from artificial seawater. Experimental results show that the adsorption characteristics of these adsorbents were dependent on the adsorbent dose, contact time, pH, stirring speed, initial TBT concentration, and temperature. Kinetic models evaluated include fractional power, pseudo-first-order, pseudo-second-order, Elovich, and intraparticle diffusivity. The kinetic data were well described by pseudo-second-order model for the adsorption of TBT onto the precursors and the composite due to their high regression coefficients. Equilibrium isotherm data were fitted using Langmuir, Freundlich, Temkin, and D–R models. Freundlich model is in good agreement with all the experimental data with high R^2 values. Thermodynamic analysis showed that the adsorption process was endothermic and spontaneous in nature. The practical application of the optimal conditions obtained for the removal of TBT from natural seawater suggests the materials as effective adsorbents for TBT removal from contaminated natural seawater; 99.7, 82.9, and 99.8% TBT was removed by the activated carbon, silica, and the composite material, respectively.

References

[1] E. Millan, J. Pawliszyn, Determination of butyltin species in water and sediment by solid-phase microextraction-gas chromatography-flame ionization detection, J. Chromatogr. A 873 (2000) 63–71.

[2] G.M. Gadd, Microbial interactions with tributyltin compounds: Detoxification, accumulation, and environmental fate, Sci. Total Environ. 258 (2000) 119–127.

[3] M.A. Sheikh, N.M. Noah, K. Tsuha, T. Oomori, Occurrence of tributyltin compounds and characteristics of heavy metals, Int. J. Environ. Sci. Technol. 4 (2007) 49–59.

[4] B. Radke, M. Staniszewska, A. Wasik, J. Namieśnik, J. Bolałek, Organotin compounds in marine sediments, Pol. J. Environ. Stud. 17 (2008) 643–654.

[5] O.S. Ayanda, O.S. Fatoki, F.A. Adekola, B.J. Ximba, Fate and remediation of organotin compounds in seawaters and soils, Chem. Sci. Trans. 1 (2012) 470–481.

[6] O.S. Ayanda, O.S. Fatoki, F.A. Adekola, B.J. Ximba, Removal of tributyltin from shipyard process wastewater by fly ash, activated carbon and fly ash/activated carbon composite: Adsorption models and kinetics, J. Chem. Technol. Biotechnol. (2013). doi: 10.1002/jctb.4088.

[7] O.S. Ayanda, O.S. Fatoki, F.A. Adekola, B.J. Ximba, Kinetics and equilibrium models for the sorption of tributyltin to nZnO, activated carbon and nZnO/activated carbon composite in artificial Seawater, Mar. Pollut. Bull. 72 (2013) 222–230.

[8] O.S. Fatoki, O.S. Ayanda, F.A. Adekola, B.J. Ximba, B.O. Opeolu, Preparation and characterization of activated carbon—nFe_3O_4, activated carbon—Silica and activated carbon—nZnO hybrid materials, Part. Part. Sys. Charact. 29 (2012) 178–191.

[9] O.S. Ayanda, O.S. Fatoki, F.A. Adekola, B.J. Ximba, Preparation and characterization of nZnO/fly ash composite, Technical Proceedings of the 2012 NSTI Nanotechnology Conference and Expo, Santa Clara, CA, 2012, pp. 95–98.

[10] O.S. Ayanda, O. Adeyi, B. Durojaiye, O. Olafisoye, Adsorption kinetics and intraparticulate diffusivities of congo red onto kola nut pod carbon. Pol. J. Environ. Stud. 21 (2012) 1147–1152.

[11] Y.S. Ho, G. McKay, A comparison of chemisorption kinetic models applied to pollutant removal on various sorbents. Trans. I Chem. E 76 (1998) 332–340.

[12] S. Azizian, Kinetic models of sorption: A theoretical analysis. J. Colloid Interface Sci. 276 (2004) 47–52.

[13] L.Y. Deng, G.R. Xu, Z.C. Yan, Q.H. Liu, G.B. Li, Removal effect of Cr (VI) by adsorbent made from sewage sludge, Water Sci. Technol. 62 (2010) 2961–2969.

[14] E. Bazrafshan, F.K. Mostafapour, M.A. Zazouli, Methylene blue (cationic dye) adsorption into Salvadora persica stems ash, Afr. J. Biotechnol. 11 (2012) 16661–16668.

[15] T.M. Alslaibi, I. Abustan, M.A. Ahmad, A. Abu Foul, Kinetics equilibrium adsorption of iron (II), lead (II), copper (II) onto activated carbon prepared from olive stone waste, Desalin. Water Treat. (2013). doi: 10.1080/19443994.2013.833875.

[16] P.S. Kumar, C. Vincent, K. Kirthika, K.S. Kumar, Kinetics and equilibrium studies of Pb^{2+} ion removal from aqueous solutions by use of nano-silversol-coated activated carbon, Braz. J. Chem. Eng. 27 (2010) 339–346.

[17] A. Gil, F.C.C. Assis, S. Albeniz, S.A. Korili, Removal of dyes from wastewaters by adsorption on pillared clays, Chem. Eng. J. 168 (2011) 1032–1040.

[18] S. Basha, Z.V.P. Murthy, Kinetics and equilibrium models for biosorption of Cr(VI) on chemically modi-

fied seaweeds. *Cystoseira indica*, Process Biochem. 42 (2007) 1521–1529.

[19] K. Ignatowicz, Selection of sorbent for removing pesticides during water treatment, J. Hazard. Mater. 169 (2009) 953–957.

[20] T. Sheela, Y. Arthoba Nayaka, R. Viswanatha, S. Basavanna, T.G. Venkatesha, Kinetics and thermodynamics studies on the adsorption of Zn(II), Cd(II) and Hg(II) from aqueous solution using zinc oxide nanoparticles, Powder Technol. 217 (2012) 163–170.